细间距器件无铅焊点力学性能和断口形貌分析

张 亮[1], 薛松柏[1], 韩宗杰[1], 禹胜林[1,2], 盛 重[1]
(1. 南京航空航天大学 材料科学与技术学院, 南京 210016;
2. 中国电子科技集团公司 第十四研究所, 南京 210013)

张 亮

摘 要: 分别采取红外再流焊和激光再流焊焊接细间距器件, 研究了 SnPb, SnAgCu 和 SnAg 三种钎料在不同焊接热源下焊点的力学性能。结果表明, 激光再流焊对应焊点的力学性能优于红外再流焊, 该现象在使用 SnAg 钎料的情况下尤为显著, 同时无铅焊点优于传统的 SnPb 焊点。对焊点断口形貌进行研究, 发现激光焊接的条件下, 焊点断口韧窝较多、较深, 断口的撕裂棱朝固定的方向延伸, 而红外热源焊接的条件下, 断口韧窝较少, 较浅, 两种情况下焊点韧窝开裂均为穿晶开裂。

关键词: 激光再流; 红外再流; 力学性能; 断口组织
中图分类号: TG456 文献标识码: A 文章编号: 0253－360X(2008)09－0035－04

0 序 言

随着电子元器件向着高密度、小型化和高可靠性方向发展, QFP(quad flat pack, 四边扁平封装)高密度组装器件的引线中心间距已达到了 0.3 mm, 单一器件上的引线数目可达到 576 条以上, 利用传统的气相再流焊、热风再流及红外再流焊等方法焊接这类细间距时, 极易发生相邻引线焊点的"桥连", 作为焊接新技术, 激光软钎焊却能很好地适用于这种高密度组装器件[1－3]。激光热源在焊接领域中的应用极为广泛[4], 由于激光热源具有可以为焊点成形提供一定的局部热源, 可以快速升温和冷却以及实现自动化等优点, 因此激光热源焊接也是电子制造行业极为有效的焊接工具[5]。在激光焊接的过程中, 热传输的过程非常复杂, Beckett 等人[6]借助有限元软件 ANSYS, 针对 QFP 器件, 对于单点、多道和脉冲激光焊接的工艺过程进行模拟, 解决了激光焊接过程热工艺的复杂性。伴随焊接方法的进步, 钎料也发生了很大变化, 由于 ROHS 和 WEEE 等禁令的出现, 国际社会对无铅钎料的呼吁也越来越强烈, SnPb 钎料的替代问题成为诸多研究人员研究的热点, 因此研究无铅钎料的焊接工艺问题凸现出来, 致使电子元器件的无铅钎料激光焊接成为目前电子封装中的一个重要发展方向。

文中选取 SnAgCu 和 SnAg 两种无铅钎料为研究对象, 以 SnPb 钎料为参考。采用红外和激光两种热源, 分别使用三种钎料焊接细间距器件。通过拉伸测试, 分析焊点抗拉强度和焊点的断口形貌。

1 试验方法

材料采用细间距器件: QFP100(引线数为 100), 引线间距为 0.5 mm。Sn-Ag-Cu 无铅焊膏: Sn-Ag-Cu 无铅钎料中, Ag 含量为(质量分数, %)3.0, Cu 含量为 0.5, 余量为 Sn。Sn-Ag 无铅焊膏: Sn-Ag 无铅钎料中, Ag 的含量为 3.5%, 余量为 Sn。Sn-Pb 焊膏: 铅的含量为 37%, 余量为锡。PCB 板: FR－4 基板, 铜表面镀锡。

设备采用 HT－990 型红外再流焊机。LY－FCDL－WS90 型半导体激光软钎焊系统。STR－1000 型微焊点强度测试仪。Quanta200 型扫描电子显微镜。

采用三种钎料, 通过红外再流焊接和半导体激光软钎焊两种焊接 QFP 器件, 焊接完成以后, 对器件进行清洗, 然后安装在微焊点强度测试仪的 45° 工作平台上, 如图 1 和图 2 所示。抗拉强度测试完成后, 采用 Quanta200 型扫描电子显微镜对拉伸断口进行分析。

收稿日期: 2008－04－11
基金项目: 江苏省普通高校研究生科技创新计划基金资助项目(CX07B－087z); 2006 年江苏省"六大人才高峰"基金资助项目(06－E－020)

图 1 微焊点测试仪

Fig. 1 Micro-joint tester

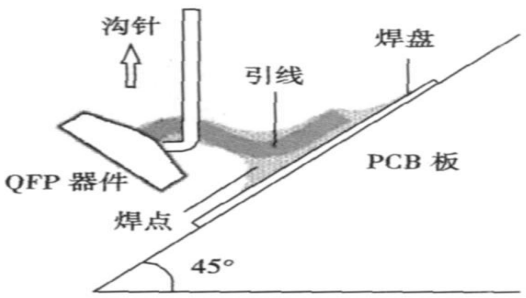

图 2 QFP 拉伸试验测试方法

Fig. 2 Tensile tests of quad flat package(QFP)

2 试验结果与分析

为了便于比较,三种钎料对应的激光再流焊接参数均为电流 16 A,焊接速度 120 mm/min。SnPb, SnAgCu, SnAg 三种焊点对应的红外回流温度峰值分别为 210, 250 和 260 ℃。对焊后器件采用 X 射线检测焊点的缺陷和焊后的形态,选择焊点良好的 QFP 器件,进行拉伸测试,图 3 为激光焊后良好器件整体效果图。

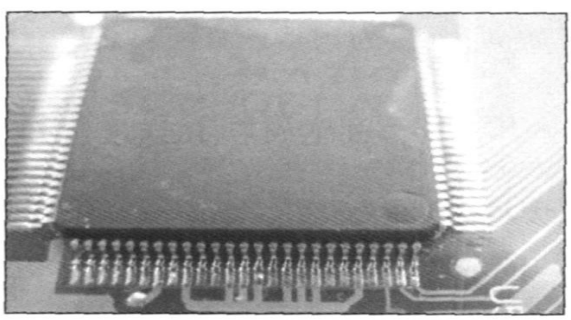

图 3 激光焊接整体效果图

Fig. 3 Schematic illustrations of QFP device after soldering

图4 为 SnAgCu 焊点在两种热源作用下焊点拉伸力曲线图,以 SnPb 焊点为参考,可以看出对于 SnAgCu 焊点激光再流焊接的情况下的焊点拉伸力大于红外热源下焊点的拉伸力,SnPb 焊点的拉伸数据也说明了激光焊接优越性,同时可以看出 SnAgCu 焊点的拉伸力大于 SnPb 焊点,说明在力学性能上,SnAgCu 焊点优于 SnPb 焊点。对 SnAg 焊点而言,图 5 也具有和图 4 类似的规律:激光再流焊接下焊点的拉伸力高于红外再流焊接,无铅焊点力学性能优于传统的 SnPb 焊点。但对于 SnAgCu/SnAg 两种钎料的激光再流焊接数据分析,发现激光再流焊接可以显著提高 SnAg 焊点强度。

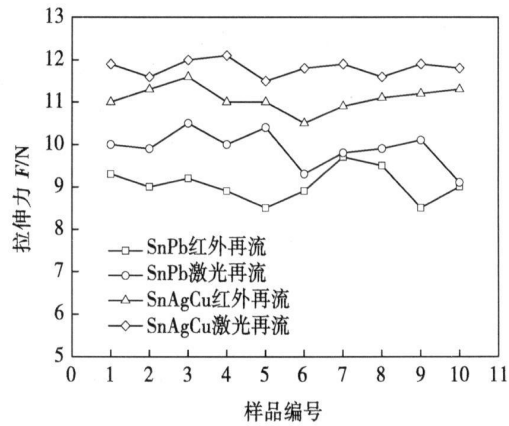

图 4 两种焊接条件下 SnAgCu/SnPb 焊点的拉伸力

Fig.4 Tensile force of SnAgCu/SnPb soldered joints with two kinds of methods

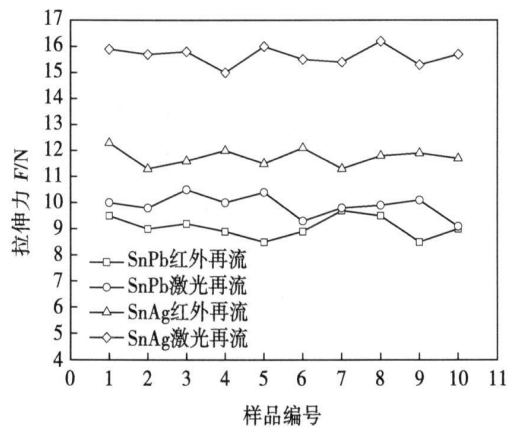

图 5 两种焊接条件下 SnAg/SnPb 焊点的拉伸力

Fig.5 Tensile force of SnAg/SnPb soldered joints with two kinds of methods

SnAgCu 合金主要由富锡相共晶组织组成,其中共晶包括二元和三元组织,二元为粒状的 Cu_6Sn_5+β-Sn,三元为针状的 Cu_6Sn_5+Ag_3Sn+β-Sn[6,7]。图 6 为对应 SnAgCu 钎料红外再流和激光再流两种不同

的加热方式下焊点断口组织。在图 6a 中可以看出红外再流加热方式下，焊点断口有一定的韧窝，且韧窝较浅，而激光再流的断口组织，图 6b 的韧窝明显更多、更深，撕裂棱朝一个方向延伸，说明激光加热的情况下，焊点在拉伸的过程中发生剧烈的塑性变形，可以断定该种断裂方式为韧性断裂。该断裂方私在相关文献也得以证实[9]。

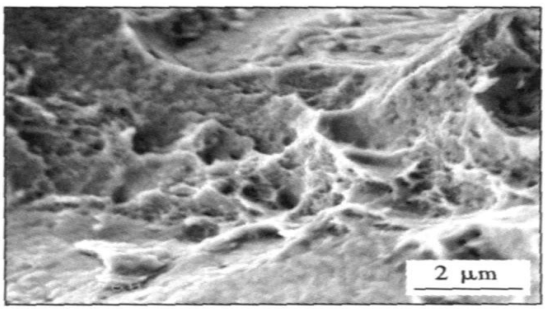

(a) 红外再流焊

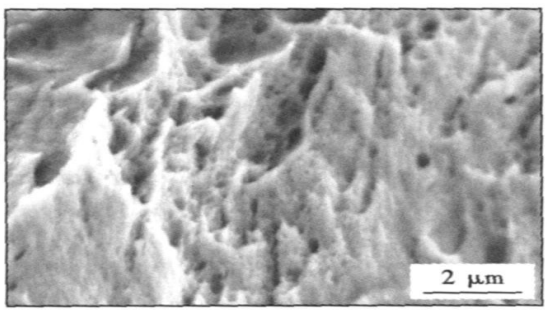

(b)　激光再流焊

图 6　QFP 器件 SnAgCu 焊点断口组织

Fig. 6　Fracture morphologies of SnAgCu soldered joints

SnPb 钎料主要由 α-Pb＋β-Sn 和 α 相或者 β 相组成，图 7a 为 SnPb 焊点在红外热源焊接的情况下的断口形貌，可以看出断口组织不均匀，呈现明显穿晶断裂的迹象，在图上可以看到有一定的韧窝存在，且分布较为弥散。图 7b 为 SnPb 焊点激光焊接条件下的断口形貌，可以看出在焊点内部出现明显的撕裂的痕迹，韧窝较为明显，说明在拉伸过程中出现较为强烈的塑性变形，因此，在拉伸过程中，焊点断裂过程以韧性断裂为主，同时发现该断裂方式符合微孔聚合型断裂特征。

SnAg 钎料也是近几年诸多研究人员研究的热点，Ridout 等人[10]借助有限元软件 PHYSICA 分析了 Sn3.5Ag 焊接片式电阻时焊点的蠕变断裂行为。Amagai 等人[11]综合分析了 SnAg 基钎料的力学性能，并进一步修正钎料的本构方程。Kim 等人[12]采用试验分析和有限元模拟两种方式分析了剪切速度

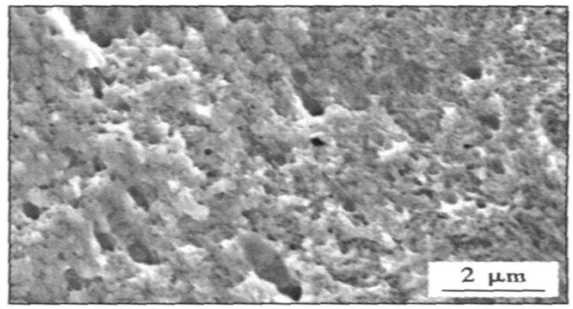

(a) 红外再流焊

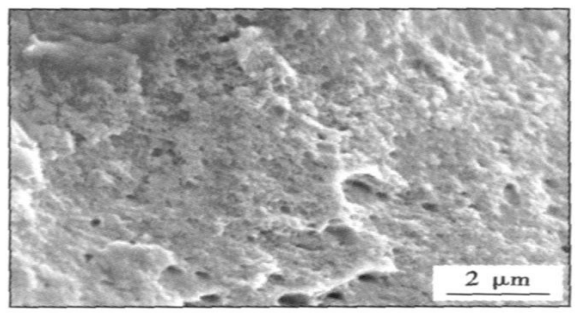

(b)激光再流焊

图 7　QFP 器件 SnPb 焊点断口组织

Fig. 7　Fracture morphologies of SnPb soldered joints

对 SnAg 和 SnAgCu 焊球的影响，相对 SnPb 和 SnAgCu 两种钎料的激光焊接，SnAg 激光焊接的研究较少。SnAg 钎料熔点为 221 ℃，该钎料具有高强度和优良的抗蠕变性能，但熔点相对偏高，成本也较高[13]。文中选择 SnAg 作为一种无铅钎料，进行激光再流焊接，图 8a 为红外热源焊接下焊点断口形貌，可以看出晶粒较为粗大，出现明显的撕裂棱，相比较图 8b 的激光焊接断口，可以发现激光再流焊接的焊点塑性变形较为明显，撕裂棱朝固定的方向延伸，韧性断裂显著。

由于焊点尺寸越来越小，焊接质量的控制就显得优为重要，而气孔、锡珠、桥连等缺陷对焊点的性能产生严重的影响[14]，而激光焊接的应用可以减少缺陷的产生，实现自动定位的微小器件的焊接[15]。针对不同的无铅钎料和电子元器件，激光参数的优化[16]、加热时间的选择[17]是激光焊接的重要内容。而可以应用的无铅钎料有很多，研究较多的是 SnAgCu 钎料，适当的控制激光焊接参数，可以使焊点外观良好，无虚焊以及桥连等缺陷的产生，对 SnPb 焊点，SnAgCu 焊点强度更高[18]，该现象和文中的研究结果吻合。Ebersberger 等人[19]研究了 SnAg 钎料应用于倒装芯片器件的激光焊接，通过测试分析，认为 SnAg 钎料可以替代 SnPb 钎料应用于大部分的电子封装器件。结合文中的研究，说明 SnAgCu，

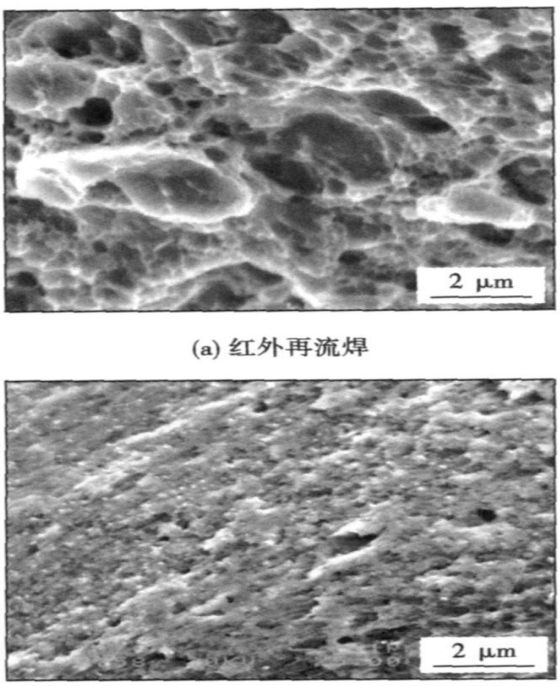

(a) 红外再流焊

(b) 激光再流焊

图 8 QFP 器件 SnAg 焊点断口组织

Fig. 8 Fracture morphologies of SnAg soldered joints

SnAg 均可以应用替代 SnPb 钎料应用于电子封装的激光焊接中。

3 结 论

(1) 在红外和激光两种热源下，选择 SnPb，SnAgCu，SnAg 三种钎料，针对细间距器件进行软钎焊试验，发现激光再流焊对应的焊点强度高于红外再流焊点强度，该现象在使用 SnAg 焊料是较为显著，同时两种无铅焊点力学性能均优于传统的 SnPb 焊点。

(2) 激光焊接情况下，焊点断口韧窝较多、较深，分布相对均匀，说明焊点在拉伸过程中呈现剧烈的塑性变形。而红外再流焊接的情况下，焊点断口组织不均匀，断口韧窝较浅。

参考文献：

[1] 黄 翔. 半导体激光对 SOP 与 CR 焊点力学性能影响的研究[D]. 南京：南京航空航天大学，2007.

[2] Raymond S D, Wild P M, Bayley C J. On modeling of the weld line in finite element analyses of tailor-welded blank forming operations[J]. Journal of Materials Processing Technology, 2004, 147(1): 28－37.

[3] 薛松柏，姚立华，韩宗杰，等. 半导体激光工艺参数对 Sn-Ag-Cu 钎料润湿性影响分析[J]. 焊接学报，2005，26(12)：39－42.

[4] 苗玉刚，陈彦宾，李俐群，等. 铝合金激光立焊特性分析[J]. 焊接学报，2007，28(10)：57－60.

[5] Beckett P M, Fleming A R, Gilbert J M, *et al*. The finite element modeling of laser soldering for electronic assemblies[J]. International Journal of Numerical Modeling: Electronic Networks, Devices and Fields, 2002, 15(3): 265－281.

[6] Beckett P M, Fleming A R, Gilbert J M, *et al*. Numbering modeling of scanned beam laser soldering of fine pitch packages[J]. Soldering and Surface Mount Technology, 2002, 14(1): 24－29.

[7] 韩宗杰，鞠金龙，薛松柏，等. 半导体激光软钎焊 Sn-Ag-Cu 焊点微观组织[J]. 中南大学学报(自然科学版)，2006，37(2)：229－234.

[8] Akio H, Hiro Y, Eiichi I, *et al*. Joint strength and interfacial microstructure between Sn-Ag-Cu and Sn-Zn-Bi solders and Cu subatrate [J]. Science and Technology of Advanced Materials, 2004, 5(2): 267－276.

[9] 姚立华. 半导体激光软钎焊技术研究[D]. 南京：南京航空航天大学，2006.

[10] Ridout S, Dusek M, Bailey C, *et al*. Assessing the performance of crack detection tests for solder joints[J]. Microelectronics Reliability, 2006, 46(12): 2122－2130.

[11] Kishimoto K, Shibuya T. Mechanical characterization of Sn-Ag based lead-free solders[J]. Microelectronics Reliability, 2002, 42(6): 951－961.

[12] Kim Jong Woong, Jung Seung Boo. Experimental and finite element analysis of the shear speed effects on the Sn-Ag and Sn-Ag-Cu BGA solder joints[J]. Materials Science and Engineering A, 2004, 371(1－2): 267－276.

[13] 张启运，庄鸿寿. 钎焊手册[M]. 北京：机械工业出版社，1999.

[14] Fidan I. CAPP for electronics manufacturing case study: fine pitch SMT[J]. Journal of Electronic Packaging, 2004, 126(1): 173－176.

[15] Beckett P M, Fleming A R, Foster R J, *et al*. An automated pick-place laser soldering process for electronics assembly[C] // Proceedings of 44th Electronic Components and Technology Conference, Washington, 1994, 1079－1081.

[16] Wang Yulin, Xiong Zhenhua, Zou Xinjue, *et al*. Experimental optimization of process parameters for diode laser soldering of BGA[C] // Conference on High Density Microsystem Design and Packaging and Component Failure Analysis, Shanghai, 2006, 171－176.

[17] 黄 翔，薛松柏，张 玲，等. 半导体激光加热时间对焊膏在铜基板上润湿铺展性能的影响[J]. 焊接学报，2006，27(11)：45－49.

[18] 张 昕. QFP 器件半导体激光无铅钎焊工艺研究[D]. 南京：南京航空航天大学，2008.

[19] Ebersberger B, Bauter R, Alexa L. Qualification of SnAg solder bumps for lead-free flip chip applications[C] // Proceedings of 54th Electronic Components and Technology Conference, Las Vegas 2004, 683－691.

作者简介：张 亮，男，1984 年出生，博士研究生。主要从事微电子焊接及无铅钎料研究。发表论文 8 篇。

Email：zhangliang@nuaa.edu.cn

to improve the performance for welder running after rolled-billet in its forward travel, reduce mechanical couplings between welder and rolled-billet, and strengthen welder's capability of withstanding disturbances from outside, a composite controller of single nerve-cell based on an artificial immune adjusting law had been applied. Simulating results show that subsection control for the welder can meet its requirements of velocity in forward travel and its requirements of displacement in return travel, a composite controller of single nerve-cell can effectively increase synchronous-precision of welder tracking rolled-billet, and the introduction of an artificial immune adjusting law in the welder driving system can obviously enhance the property of welder resisting outside disturbances.

Key words: flash-butt welder; virtual prototype; composite control; artificial immune adjusting law

Effect of Ni on wettability and shear strength of joints of Ag20CuZnSnP filler metal LI Zhuoran, LIU Bin, FENG Jicai (State Key Laboratory of Advanced Welding Production Technology, Harbin Institute of Technology, Harbin 150001, China). p19—22

Abstract: By adding different content of Ni into the Ag20CuZnSnP filler metal, the effect of Ni on wettability and the shear strength of joints are studied and analysed. The results indicate that when the content of Ni is more than 2.0%, the area of wettability on stainless steel is improved obviously; when the content of Ni is 2.0%, the maximum of the shear strength is attained. The analysis of microstructure of filler metals indicate that the size of tin bronze becomes small when the element of Ni is added into the filler metal and the existence of Ni is Ni_3P in which element P is took by Ni from the compound of Cu_3P.

Key words: filler metal; wettability; shear strength of joint; microstructure; Ni

High frequency brazing of 0Cr18Ni9Nb to YG6 using Cu-based microcrystalline brazing alloys ZHAI Qiuya[1], LIANG Cunkun[1,2], CHENG Jun[1], XU Jinfeng[1] (1. Materials Science and Engineering, Xi'an University of Technology, Xi'an 710048, China; 2. Gree Electric Appliances, Inc. of Zhuhai, Zhuhai 519070, Guangdong, China). p23—26

Abstract: The high frequency brazing of 0Cr18Ni9Nb stainless steel to YG6 cemented carbide was conducted by using Cu-*x*wt% Sn (*x* = 7, 13.5) microcrystalline brazing alloys, and the phase constitution, microstructural morphology and interfacial element distribution characteristics of brazing joint were investigated. The relationship between the microstructure of joint and the composition of brazing alloy together with atom mutual diffusion behavior was analyzed. The experimental results show that the Cu-based microcrystalline brazing alloys perform an excellent wettability and spreadability in induction brazing process. Owing to the atom mutual diffusion between the liquid Cu-based brazing alloys and the base metal to a certain extent, the metallurgical bonding of 0Cr18Ni9Nb to YG6 has achieved. The joint microstructure is dense and homogeneous, which has no defects such as slag inclusion and porosity etc. The microstructure of brazing seam consists mainly of α-Cu solid solution and a few of intermetallic compounds in the 0Cr18Ni9Nb/ Cu-*x*wt% Sn/YG6 joint, and the quantity of intermetallic compounds increases with the rise of Sn content. The base metals near the interface have no obvious coarsening appearance.

Key words: microcrystalline brazing alloy; high frequency brazing; interface; joint microstructure

Impulse pressuring diffusion bonding of titanium alloy to stainless steel with nickel interlayer YUAN Xinjian, SHENG Guangmin, QIN Bin, HUANG Wenzhan (College of Materials Science and Engineering, Chongqing University, Chongqing 400044, China). p27—30

Abstract: Titanium alloy TA17 and austenitic stainless steel 0Cr18Ni9Ti were bonded by using impulse pressuring diffusion bonding (IPDB) with nano nickel particles, nano nickel plating and pure nickel foil as a interlayer, respectively, and the tensile strength of bonded joint was tested. The bonding strength of the joint bonded by using the three types of nickel interlayer metals has reached as high as 212 MPa, 175 MPa and 334 MPa, respectively. The properties of the bonded joint using pure nickel foil are clearly better than the joints obtained by nano nickel particles and nano nickel plating. The fracture appearances were observed and analyzed by metallographic microscope. Element distribution and phase structures of each joint zone were analyzed by scanning electron microscope (SEM) and energy dispersive spectroscopy (EDS) and X-ray diffraction (XRD). The results show that the density of the nano nickel particles interlayer is not high enough, the quality of the plating interlayer of nano nickel is not good enough which limited the increase of the joint strength, but Ni interlayer has successfully inhibited interdiffusion of Fe and Ti and avoided forming Fe-Ti series intermetallics.

Key words: titanium alloy; stainless steel; nickel interlayer; impulse pressuring; diffusion bonding

Welding arc load characteristics of variable polarity TIG welding and its control strategy at commutation DING Kun[1,2], YAO Heqing[1], FAN Xinghui[1], WANG Shouyan[1] (1. College of Mechanical & Electrical Engineering, Hohai University, Changzhou 213022, Jiangsu, China; 2. College of Electrical Engineering, Hohai University, Nanjing 210098, China). p31—34

Abstract: Welding arc load characteristics of variable polarity TIG welding was studied through experiment. The experimental results indicate that equivalent resistance of welding arc in EN is less than it in EP, both of them decrease as increasing of welding current, the equivalent resistance will drop rapidly at the time when EP commutate to EN. The mechanism of equivalent resistance analyzed is concerned with the working mechanism of negative, arc column and anodic at different load current. A control strategy incorporate variable parameter PI into advance control is presented to solve the problem of vary equivalent resistance at the time EP commutate to EN. Experimental results prove this control strategy is available.

Key words: variable polarity; equivalent resistance; thermionic emission; advance control

Investigation of mechanical property and fracture morphology of lead-free soldered joints of fine pitch devices ZHANG Liang[1], XUE Songbai[1], HAN Zongjie[1], YU Shenglin[1,2], SHENG Zhong[1] (1. College of Materials Science and Technology, Nanjing U-

niversity of Aeronautics and Astronautics, Nanjing 210016, China; 2. The 14th Research Institute, China Electronics Technology Group Corporation, Nanjing 210013, China). p35—38

Abstract: Soldering experiments of fine pitch devices were carried out using diode-laser soldering system and IR reflow soldering with SnPb, SnAgCu, SnAg, and the tensile strengths of soldered joints were measured by Micro-joints Tester. The results indicate that mechanical properties of fine pitch devices soldered joints with laser soldering system is better than that of fine pitch devices soldered joints with IR reflow soldering method, especially for SnAg soldered joints, and the mechanical properties of lead-free soldered joints is also better than that of Sn-Pb solder. The characteristics of fracture morphology of micro-joints were also analyzed by SEM. It is found that the fracture mechanism of micro-joints soldered with laser soldering system is toughness fracture, and mangled edges appear in a fixed direction. While the fracture morphology of micro-joints soldered with IR reflow soldering method has less and lower dimples than that with diode-laser soldering system. Both the dimple crack mechanisms under the wow soldering methods belong to transgranular crack.

Key words: diode-laser reflow; IR reflow; mechanical properties; fracture morphology

Effect of geometrical parameters of coil on electromagnetic force in coil-sheet system XU Wei, LIU Xuesong, YANG Jianguo, FANG Hongyuan (State Key Laboratory of Advanced Welding Production Technology, Harbin Institute of Technology, Harbin 150001, China). p39—42, 54

Abstract: Based on the new idea of controlling welding stress with trailing electromagnetic force, the electromagnetic force in flat spiral coil-aluminum sheet system was simulated with finite element software ANSYS. Effect of geometrical parameters of coil on electromagnetic force was analyzed. The results show that the electromagnetic force acts on the location where the coil projects on the sheet. With decreasing outer diameter of the coil, the electromagnetic force peak magnitude increases and the peak position of the axial force moves linearly close to the inner side of coil. With increasing inner diameter, the radial force peak magnitude increases, the axial force peak magnitude increases first and then decreases, and the peak position of the axial force is fixed first and then moves close to outer side of coil. With increasing wire width, the electromagnetic force magnitude increases. The variation of the position, where the direction of the radial force is turned, with the inner and outer radius is similar to that of the peak position of the axial force. While controlling welding stress based on electromagnetic force, the coil with the smaller outer radius and the appropriate inner radius should be selected, and the magnetic medium is needed to enhance electromagnetic force.

Key words: electromagnetic force; geometrical parameters; flat spiral coil; welding stress

Microstructure and properties of TiC reinforced composite coating fabricated on Ti alloy by GTAW WANG Zhenting[1, 2], CHEN Lili[2], ZHANG Xianyou[1] (1. Mobile Postdoctoral Center of Materials Science and Engineering, Harbin University of Science and Technology, Harbin 150080; 2. College of Materials Science and Engineering, Heilongjiang Institute of Science and Technology, Harbin 150027, China). p43—45

Abstract: A metal matrix composite coating reinforced by TiC particulates has been successfully fabricated utilizing the in-situ reaction of pre-placed C powder on Ti alloy by gas tungsten arc welding (GTAW) process. The microstructure of the coating was analyzed by scanning electron microscopy (SEM), X-ray diffraction (XRD) and energy-dispersive spectrum (EDS). The growing mechanism of TiC was discussed. Microhardness and wear resistance at room temperature of the composite coating were examined by means of Microhardness Tester and Wear Tester respectively. The results show that microstructure of the composite coating is uniform and the fine TiC exhibites dendrite and strip shapes. The composite coating reinforced by in-situ TiC apparently improves surface hardness of Ti alloy, the average microhardness can reach HV700, and its gradient distribution appears. Wear resistance of the composite coating is about 10.5 times of Ti alloy's substrate.

Key words: Ti alloy; GTAW; in-situ synthesis; coating; microstructure

Residual stress field in hole-drilling method—part I: Theoretical analysis LI Hao, LIU Yihua (School of Civil and Hydraulic Engineering, Hefei University of Technology, Hefei 230009, China). p46—50

Abstract: During the residual stress measurement by using the hole-drilling method, a work-hardening layer near the hole will be formed due to the cutting force. As the material characteristics in the work-hardening layer will vary evidently, the layer surrounding the hole can affect the stress relieved after hole drilling. The work-hardening layer was simplified as a heterogeneous annulus by increasing the elastic modulus of the material near the hole, and the analytical solution of the release stresses after drilling in a infinite plate submitted to the biaxial uniform stresses was developed by using the method of elasticity. The release stresses in a 304 stainless steel plate under the biaxial stresses were numerically calculated by the FEM program MSC/Patran &Nastran and compared with the analytical solution. The results indicate that the simplified model is feasible and the analytical solution is valid. When the residual stresses are determined by using the hole-drilling method, it will be more accurate if the work-hardening layer is considered.

Key words: residual stress; hole-drilling method; work-hardening; modulus of elasticity; analytical solution

Abradability of Cu-Al_2O_3 gradient coatings by plasma spraying LI Gaohong[1, 2], FENG Lajun[1], LEI A-li[1], XU Dapeng[1] (1. School of Materials Science and Engineering, Xi'an University of Technology, Xi'an 710048, China; 2. School of Materials and Chemical Engineering Xi'an Technological University, Xi'an 710032, China). p51—54

Abstract: Cu-Al_2O_3 gradient coatings were prepared by plasma spray. The microstructure and abraded superficial shape of the coatings were analyzed by metallomicroscopy and SEM. The wear-resisting property of Cu-Al_2O_3 gradient ceramic coatings was tested by self-produce immobile wearing machine. The results show that the